Comments on phase-front propagation in ferroelectrics

1994 J. Phys.: Condens. Matter 6 3583

(http://iopscience.iop.org/0953-8984/6/19/014)

J. Phys.: Condens. Matter 6 (1994) 3583–3591. Printed in the UK

Comments on phase-front propagation in ferroelectrics

J A Tuszyński† and D Sept†
Institut für Theoretische Physik I, Heinrich-Heine Universität Düsseldorf, D-40225 Düsseldorf, Germany

Received 30 December 1993, in final form 21 February 1994

Abstract. We examine a model of interface motion in ferroelectrics and find new solutions in addition to those presented recently by Gordon. We then apply our results to analyse the experimental data obtained for $PbTiO_3$ by Dec. Good qualitative agreement has been found between experiment and theory.

1. Introduction

Interface motion in ferroelectrics and antiferroelectrics [1–5], as well as ferromagnets [6–8] has been the object of extensive experimental and theoretical studies [9–11] in recent years. This topic of current interest is important as a means of probing multistable dynamical systems and also as a challenging example of non-linear behaviour.

A recently published study of phase-front motion in the ferroelectric $PbTiO_3$ crystal [4] revealed several peculiarities which warrant a theoretical inquiry into the underlying physical mechanisms. In particular, two distinct types of phase boundary motion were observed:

(a) rapid motion at an approximately constant velocity which takes place over short periods of time;

(b) slow motion that can be described by a cubic polynomial dependence of position on time. This type of motion persists over longer periods of time (Δt) up to a critical velocity v_c which is virtually independent of the temperature gradient across the sample.

Our objective in this paper will be to analyse theoretically the experimental data of Dec [4] within a recently proposed model of Gordon [9]. We believe that Gordon's model captures most of the essential physical characteristics for phase boundary motion in a ferroelectric undergoing a first-order phase transition. However, a subsequent analysis of solutions to the derived equations is, in our opinion, insufficient and misses several key points. It will be our goal to extend Gordon's analysis so that direct contact with experimental findings can be made.

2. The theoretical model

The starting point in Gordon's model [9] is to postulate a Landau–Ginzburg-type free-energy expansion for the ferroelectric crystal in the form

$$F = F_0 + \frac{1}{2}AP^2 - \frac{1}{4}BP^4 + \frac{1}{6}CP^6 - \frac{1}{2}e\sigma P^2 - \frac{1}{2}s_0\sigma^2 + D\left(\frac{\partial P}{\partial x}\right)^2 \qquad (1)$$

† Permanent address: Department of Physics, University of Alberta, Edmonton, Alberta, T6G 2J1, Canada.

0953-8984/94/193583+09$19.50

where P is the spontaneous polarization, $B > 0$, $C > 0$ are constant expansion coefficients, $A = a(T - T_0)$, and T_0 is the temperature at which the paraelectric phase loses its stability. Here, $D > 0$; σ is the mechanical stress that couples with P^2 due to the piezoelectric effect.

To describe the time evolution of the order parameter P, a time-dependent Landau–Ginzburg equation is then derived [9] which takes the form

$$\frac{\partial P}{\partial t} + \Gamma(AP - BP^3 + CP^5 - e\sigma P) - 2\Gamma D\frac{\partial^2 P}{\partial x^2} = 0. \tag{2}$$

This is coupled to the mechanical deformation which is found by minimizing F with respect to σ, i.e.

$$\epsilon = -\frac{\partial F}{\partial \sigma} = \frac{1}{2}eP^2 + s_0\sigma. \tag{3}$$

Since $\epsilon = \partial u/\partial x$ is the strain tensor component corresponding to σ, it also satisfies the wave equation of an elastic medium whose density is ρ:

$$\rho\frac{\partial^2 \epsilon}{\partial t^2} = \frac{\partial^2 \sigma}{\partial x^2}. \tag{4}$$

Substituting ϵ from equation (3) into equation (4) yields

$$\frac{\partial^2}{\partial t^2}\left[\frac{\rho e}{2}P^2 + \rho s_0\sigma\right] = \frac{\partial^2 \sigma}{\partial x^2} \tag{5}$$

which, together with equation (2), forms the basic system of coupled differential equations on P and σ derived and discussed by Gordon [9]. While the derivation itself is very ingenious and physically well thought out, the analysis that followed in [9] was, perhaps, too restrictive since only a limited number of special solutions were found, some of which had features that require extra care and attention. In the section that follows we present an extended analysis of the system of equations (2) and (5).

3. Analysis of solutions

Firstly, we rewrite equation (5) as

$$\frac{\rho e}{2}\frac{\partial^2}{\partial t^2}(P^2) = \left(\frac{\partial^2}{\partial x^2} - \rho s_0\frac{\partial^2}{\partial t^2}\right)\sigma \tag{6}$$

which allows four distinct possible sets of solutions. The four *ansätze* that we propose are listed below.

(i) $\sigma = \sigma(x \pm ut)$ where σ is an *arbitrary* function of $\xi = x \pm ut$ provided the velocity of propagation is $u = (\rho s_0)^{-1/2}$, i.e. the velocity of sound. Simultaneously, the polarization variable satisfies $P^2 = f(x) + \alpha t$ where f is an *arbitrary* function of x and α is an arbitrary constant.

(ii) $\sigma =$ constant and P is given as above.

(iii) Both σ and P are functions of the same (moving coordinate) variable $\xi = x \pm vt$, so that equation (6) can be readily integrated to yield

$$\frac{\rho e}{2}v^2P^2 - (1 - \rho s_0 v^2)\sigma = c_1\xi + c_0 \tag{7}$$

which becomes the solution derived by Gordon [9] provided $c_1 = c_0 = 0$. We believe that letting c_1 and c_0 be non-zero may have physical consequences and the arbitrary assumption that they vanish is not justified. However, in the present paper we will not make direct comparison between these valid solutions and experimental results.

(iv) If $\sigma = \sigma(t)$, then

$$\frac{\rho e}{2} P^2 = \sigma + c_0 + c_1 t + f(x) \tag{8}$$

where c_0 and c_1 are arbitrary constants and f is an arbitrary function of x.

What we have done so far is to solve equation (5) independently of equation (2). Obviously, we must now return to equation (2) with these four special types of solution, eliminate those that contradict it and specify those that satisfy it to such a form that full consistency is achieved. We realise that the analysis we present here is not entirely general and the problem merits a more advanced mathematical investigation. Our objective, however, is to capture the essential physical behaviour.

Another comment which is worth noting is that this model can be applied to both first- and second-order phase transitions. In the latter case we could simply require that $C = 0$ and take a negative value for B.

Below, we discuss the results of substituting the solutions of equation (5), itemized in (i)–(iv), into equation (2) and checking for consistency.

(i) With $\xi = x \pm ut$, $\sigma = \sigma(\xi)$ and $P^2 = f(x) + \alpha t$ we obtain

$$2\alpha(f + \alpha t) + 4\Gamma A(f + \alpha t)^2 - 4\Gamma B(f + \alpha t)^3 + 4\Gamma C(f + \alpha t)^4 - e\sigma(\xi)(f + \alpha t)^2 - 4\Gamma D f''(f + \alpha t) - 2\Gamma D(f')^2 = 0 \tag{9}$$

where

$$f' = \partial f / \partial x.$$

The above equation appears to be solvable only for σ in the form of a standing wave, i.e. $u = 0$, and hence also $\alpha = 0$. This would then reduce to

$$4\Gamma A f^2 - 4\Gamma B f^3 + 4\Gamma C f^4 - e\sigma_0(x) f^2 - 4\Gamma D f'' f - 2\Gamma D(f')^2 = 0 \tag{10}$$

which is solvable numerically for an arbitrarily given profile of $\sigma_0(x)$. Figure 1 shows two sample profiles, one in the form of a periodic stress wave and another taken to be a front.

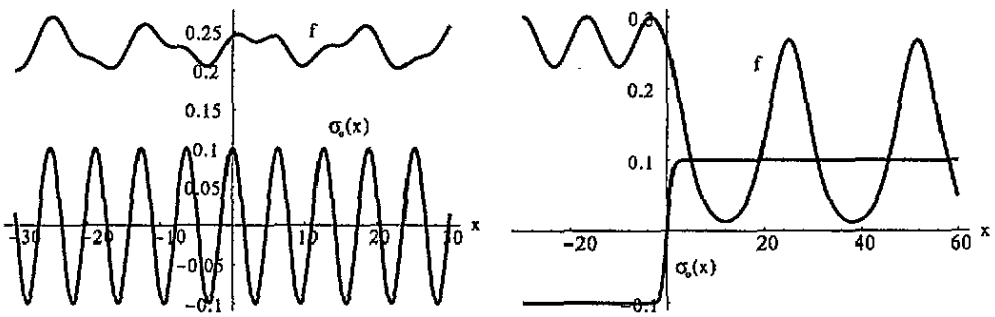

Figure 1. Plot of solution $f(x)$ to equation (10) assuming that (a) the stress pattern $\sigma_0(x)$ is periodic, (b) $\sigma_0(x)$ is a front.

Letting $u \neq 0$, i.e. introducing a propagation velocity to the stress wave, requires the polarization wave to also propagate at the same speed. Hence, $f(x) = x$ and $\alpha = u$. This yields a particular solution for $\sigma(\xi)$, i.e.

$$\sigma(\xi) = \frac{1}{e\xi^2}\left[2u\xi + 4\Gamma A\xi^2 - 4\Gamma B\xi^3 + 4\Gamma C\xi^4 - 2\Gamma D\right] \tag{11}$$

which is singular at the point $\xi = 0$ and hence may be interpreted as a propagating point defect which may represent a localized lattice contraction (see figure 2). Simultaneously, the associated polarization function diverges at large x. This either means that the entire solution is not physical or its spatial validity is limited to a finite range.

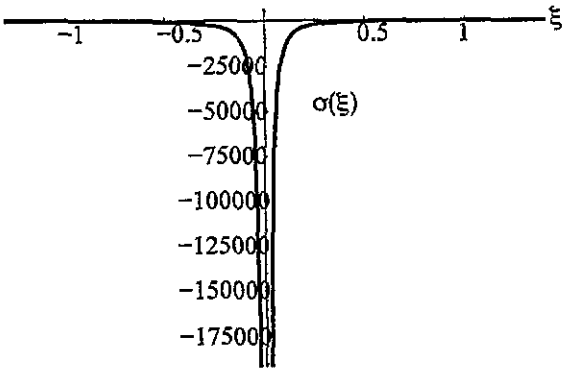

Figure 2. Solution of equation (11) representing a defect $\sigma(\xi)$.

(ii) for $\sigma = \sigma_0 =$ constant we obtain the usual time-dependent Landau–Ginzburg (TDLG) equation for the polarization wave $P(x, t)$:

$$\frac{\partial P}{\partial t} - 2\Gamma D\frac{\partial^2 P}{\partial x^2} + \Gamma[(A - e\sigma_0)P - BP^3 + CP^5] = 0. \tag{12}$$

This equation has been recently analysed from the point of view of symmetry reduction [12]. In one-dimensional space, propagating solutions exist in the form $P(x, t) = \rho(x)f(\xi)$ where, in general, $\rho(x) = 1$, $\xi = x - vt$ with an arbitrary velocity v. However, in the special case of critical and tricritical points *accelerating* solutions were found for which $\rho(x) = x^{-1/2}$, $\xi = t/2x^2$ if $A = B = 0$ (tricritical point) and $\rho(x) = x^{-1}$, $\xi = t/2x^2$ if $A = C = 0$ (critical point).

Note that in equation (12), the effect of coupling to the mechanical stress (stationary) is equivalent to a shift in the characteristic temperatures, e.g.

$$T_0 \to T_0 + \frac{e\sigma_0}{a}. \tag{13}$$

The form of solutions to equation (12) has been discussed at length elsewhere [13] and is, in general, of a damped-oscillatory type (see figure 3(a)) unless it becomes a kink (see figure 3(b)) provided the velocity of propagation v satisfies a specific relationship which is discussed later (see equation (22)) [14]. The important thing to note is that interface fronts propagate at a *specific* velocity given by the magnitude of stress σ_0 and the temperature T. We will come back to this point later when we analyse the experimental situation.

(iii) In this case we have the relationship between σ and P given by equation (7) which, when substituted into equation (2), yields

$$-vP' + \Gamma(\tilde{A}P - \tilde{B}P^3 + CP^5) - 2\Gamma DP'' = 0 \tag{14}$$

where

$$P' = \partial P/\partial\xi$$

and the renormalized expansion coefficients are

$$\tilde{A} = A - ec_0 - ec_1\xi \tag{15}$$

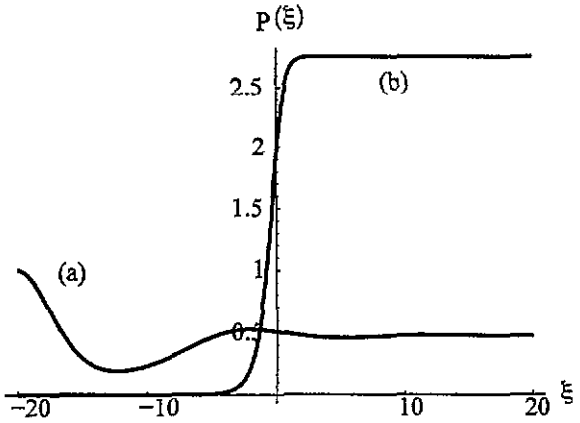

Figure 3. Two types of propagating solution $P(\xi)$ to equation (12): (a) damped oscillatory profile and (b) a kink.

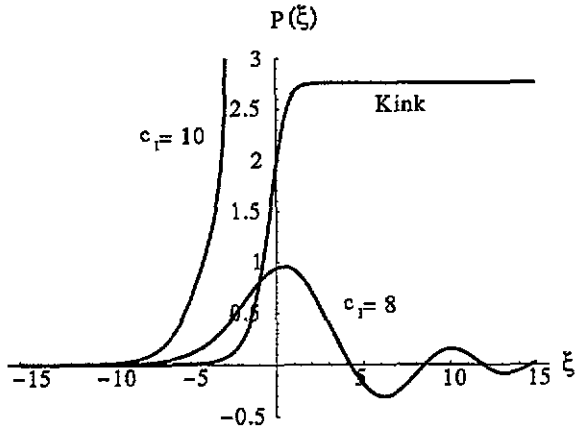

Figure 4. Solution of $P(\xi)$ for equation (14) with $c_1 = 8$, 10 compared with kink solution.

and

$$\tilde{B} = B + \frac{\rho e v^2}{2(1 - \rho s_0 v^2)}. \tag{16}$$

Several observations can be made on the basis of the above equation. First, for sufficiently high velocity values, an effective cross-over region from first- to second-order phase-transition dynamics can be obtained. This means that with $B > 0$, $\tilde{B}$ becomes negative provided

$$v^2 \geqslant \frac{2B}{2B\rho s_0 - \rho e} \equiv v_c^2. \tag{17}$$

Note that the critical velocity v_c is independent of temperature. Second, the effect of coupling to stress is, in addition to the above, to (a) renormalize the characteristic temperatures due to c_0, and (b) sharpen the boundary profile due to c_1. The latter effect can be seen as deepening the local potential well with an increase of ξ. Eventually, for a large enough ξ a singularity in P will develop causing rupture in the crystal, simultaneously with $\sigma \to \infty$ as $\xi \to \infty$. In figure 4 we have shown the effect of c_1 on a typical step-like solution.

Finally, it is perhaps worth mentioning that assuming $\tilde{B} < 0$, in particular for second-order phase transitions, requires some minor modifications but can still be incorporated in this analysis.

If $c_1 = c_0 = 0$ as assumed by Gordon [9], we then simply have

$$2\Gamma D P'' + vP' - \Gamma(AP - \tilde{B}P^3 + CP^5) = 0. \tag{18}$$

This equation has an exact kink-like solution in the form [9]

$$P = \frac{P_f}{\sqrt{2}}\left[1 + \tanh\left(\frac{\xi}{2\Delta}\right)\right]^{1/2} \tag{19}$$

where P_f is

$$P_f^2 = \frac{\tilde{B}}{2C}\left[1 + \sqrt{1 - \frac{4AC}{\tilde{B}^2}}\right] \tag{20}$$

and the width

$$\Delta = \sqrt{\frac{3D}{2[\tilde{B}P_f^2 - A]}} \tag{21}$$

moving with a velocity given by the equation

$$v = \frac{2}{3}\Gamma\Delta(4A - \tilde{B}P_f^2). \tag{22}$$

This model implies a velocity selection mechanism given mathematically by the formula above. Note that Gordon's equations for P_f, Δ and v are very similar (a few misprints can easily be corrected by comparison with our equations (20)–(22)), but still keep the dependence on σ which is decoupled in our paper. In this respect, Gordon's analysis is incomplete since σ is an independent variable just like P is. We wish to emphasize that both P_f and Δ are strongly velocity dependent through $\tilde{B}$ and hence equation (22) is only implicit. Lastly, the above formulae can be easily recalculated in the case of second-order phase transitions where different sign conventions result in minor changes.

4. Comparison with experiment

In his experimental work on $PbTiO_3$ phase-front dynamics, Dec [4] identified two distinct regions of behaviour. Slow phase-front movement over a distance Δx in a time Δt can be fitted with a cubic equation for distance ξ as a function of t, i.e.

$$\xi = a_1 t + a_2 t^2 + a_3 t^3 \tag{23}$$

and hence

$$v = \frac{d\xi}{dt} = a_1 + 2a_2 t + 3a_3 t^2. \tag{24}$$

In figure 5(b) we have shown the plots of $v(\xi)$ for the seven sets of data listed in table 1 of [4]. We have reproduced the essential parts of this table in our table 1 for easy reference. Rapid phase-front motion over a distance $\Delta x'$ in a very short interval $\Delta t'$ is characterized by a constant propagation velocity.

We believe that the slow phase-front dynamics can be directly described using the extended model of Gordon that was presented in section 3 of our paper. To this end we have analysed v in our equation (22) as a function of position ξ. Note that the experimental conditions involved the presence of a temperature gradient across the sample $\Delta T/\Delta x$ whose

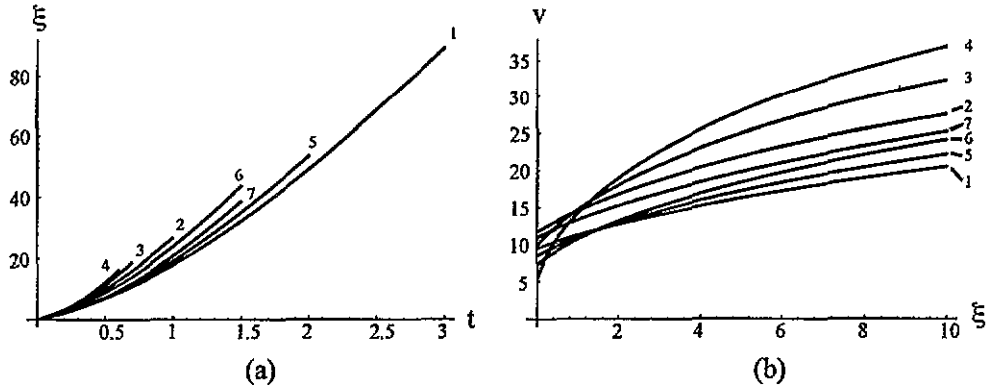

Figure 5. Plots of (a) $\xi(t)$; (b) $v(\xi)$. Labels correspond to the seven experimental sets of data given in table 1.

three values used were 4.0, 2.5 and 1.5 K mm^{-1}. The presence of a temperature gradient is required for phase-front propagation since the experiment involved is a first-order phase transition in which there exists a potential barrier between the two coexisting phases. Obviously, second-order phase transitions are characterized by a different behaviour. In terms of the model parameters, only the coefficient A is assumed to depend on temperature, i.e. $A = a(T - T_0)$. The presence of a uniform temperature gradient across the sample implies that

$$T(\xi) = (\Delta T/\Delta x)\xi + T_1 \tag{25}$$

where T_1 is the temperature at the reference end for which $\xi = 0$. Consequently,

$$A(\xi) = a\Big((\Delta T/\Delta x)\xi + T_1 - T_0\Big). \tag{26}$$

We have assumed the above linear dependence of $A(\xi)$ and studied numerically its implications on the plot $v(\xi)$ from the theoretical expression in equation (22). Figure 6 shows our findings with respect to the variation of several key model parameters:

(a) changing C affects the plot of $v(\xi)$ rather negligibly;

(b) changing e has little effect on $v(\xi)$;

(c) changing B has some effect on the initial velocity v_0 but little effect on the shape of the plot or the asymptotic velocity;

(d) a variation in the temperature gradient coefficient $\Delta T/\Delta x$ has no visible effect on the initial velocity v_0, i.e. the intercept on the diagram is virtually unaffected, while it alters very substantially the plot $v(\xi)$. This is in total agreement with the experimental findings where v_1 did not depend on $\Delta T/\Delta x$ but the form of $v(\xi)$ varied.

We, therefore, claim good qualitative agreement between the model presented here and the slow-front dynamics. Figure 7 illustrates that our theoretical results can be closely fitted to the experimental curves. However, we do not believe that the fast-front dynamics is described by the same solution of the coupled equations of motion. The fact that these fast movements do not depend on the temperature gradient indicates possibly a different type of solution. As stated by Dec [4], fast motion is connected to the detachment of the phase-front from the dislocation network. This can be translated into a decoupling between $P(\xi, t)$ and $\sigma(\xi, t)$. One such possibility exists under our item (ii) where the stress wave is stopped altogether (for example by a defect) while the polarization wave P satifies the rescaled

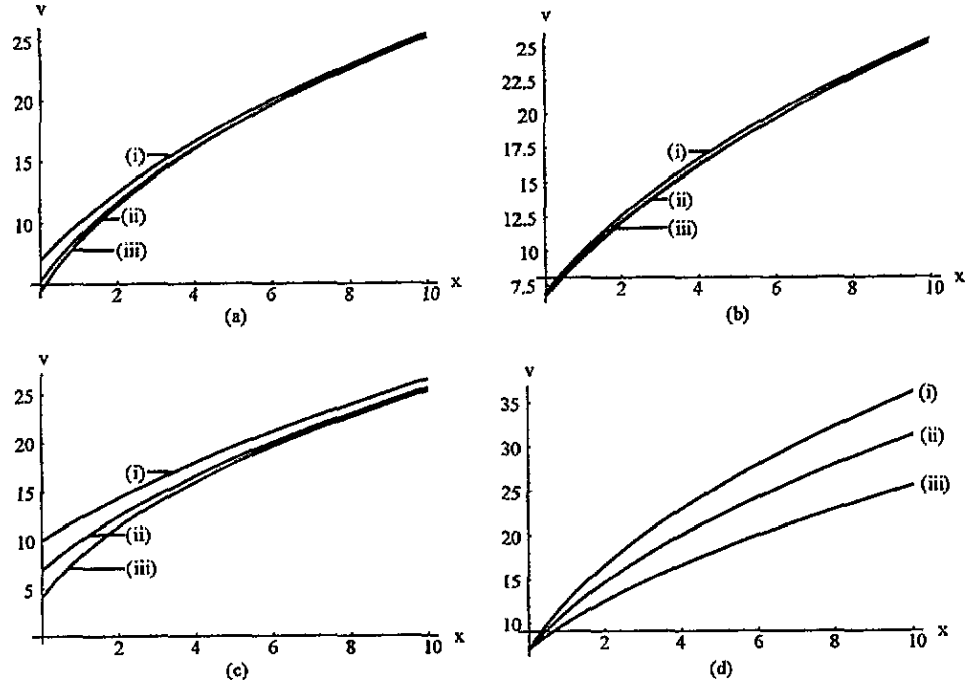

Figure 6. Plots of $v(\xi)$ based on numerical solutions to equation (22) for (a) different values of C. C = (i) 1, (ii) 3, and (iii) 5; (b) different values of e, e = (i) 0.05, (ii) 0.1, and (iii) 0.5; (c) different values of B, B = (i) 1, (ii) 3, and (iii) 5; and (d) different values for $\Delta T/\Delta x$ = (i) 2, (ii) 1.5, and (iii) 1.

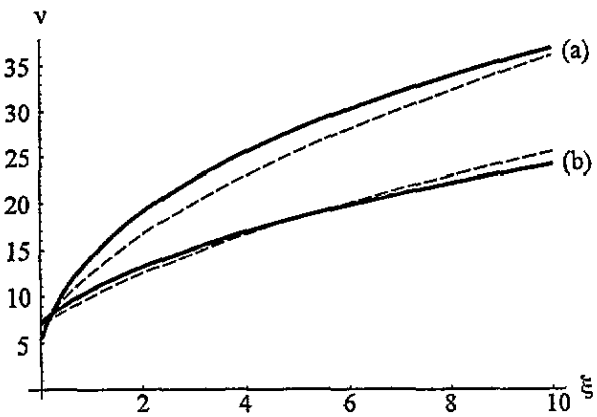

Figure 7. Fits of experimental (solid) to theoretical (dashed) curves for (a) data set 4 and (b) data set 6 in table 1.

TDLG equation. Note that here a substantial amount of mechanical stress may overshadow the temperature-dependent coefficient A in equation (12) resulting in a virtually constant-velocity propagation of the polarization wave. The velocity propagation in this case is a function of Γ, D, B, and σ_0.

Table 1. Experimental values of the model parameters following [4].

No	$\Delta T/\Delta x$ (K mm^{-1})	a_1 (μm s^{-1})	a_2 (μm s^{-2})	a_3 (μm s^{-3})	Δt (s)
1	4.0	9.5	9.2	−0.8	2.93
2	4.0	11.7	19.1	−4.0	0.94
3	4.0	9.9	30.5	−8.6	0.69
4	4.0	5.4	45.9	−15.4	0.56
5	2.5	8.5	12.2	−1.5	1.92
6	2.5	7.3	15.7	−2.2	1.44
7	1.5	11.0	14.3	−1.4	1.43

5. Summary

This paper has been concerned with the modelling of phase-front propagation in ferroelectrics. We adopted the model proposed by Gordon [9] where the spontaneous polarization (order parameter) is coupled to a stress wave. We analysed the equations of motion derived by Gordon and found several types of solution, both old and new. The old solutions in the form of moving kinks were found to be explicitly expressible in terms of model parameters, in particular, the propagation velocity. Several new types of solution were also obtained, some of which may represent defect structures and some others allow for an independent motion of stress and polarization waves. Finally, we made a direct comparison of this model with the experimental results of Dec [4] for $PbTiO_3$. Kink-type phase-front motion provided a model for slow-velocity behaviour while decoupled dynamics of P and σ appears to be consistent with the fast phase-front motion observed.

Acknowledgments

This research was supported by grants from NSERC (Canada), Deutscher Akademischer Austauschdienst, and the Alexander von Humboldt Foundation.

References

[1] Dec J 1986 *Ferroelectrics* **69** 181
[2] Fesenko E G, Martynenko M A, Gavrilyatchenko V G and Semenchev A F 1975 *Izv. Akad. Nauk. Ser. Fiz.* **39** 762
[3] Yufatova S M, Sindeyev Yu G, Gavrilyatchenko V G and Fesenko E G 1980 *Ferroelectrics* **26** 809
[4] Dec J 1988 *J. Phys. C: Solid State Phys.* **21** 1257
[5] Dec J and Yurkevich V E 1990 *Ferroelectrics* **110** 77
[6] Bulaevskii L W and Ginzburg V L 1964 *Sov. Phys.–JETP* **18** 530
[7] Khan W I and Melville D 1983 *J. Magn. Mater.* **36** 265
[8] Winternitz P, Grundland A M and Tuszyński J A 1988 *J. Phys. C: Solid State Phys.* **21** 4931
[9] Gordon A 1991 *Phys. Lett.* **154A** 79
[10] Gordon A and Salditt T 1992 *Solid State Commun.* **82** 911
[11] Gordon A, Vagner I D and Wyder P 1993 *Physica* B **191** 210
[12] Skierski M, Grundland A M and Tuszyński J A 1989 *J. Phys. A: Math. Gen.* **22** 3789
[13] Tuszyński J A, Otwinowski M and Dixon J M 1991 *Phys. Rev.* B **44** 9201
[14] Gordon A 1983 *Phys. Lett.* **99A** 329